Comparison Study between SVM and PWM Inverter in Sliding Mode Control of Active and Reactive Power Control of a DFIG for Variable Speed Wind Energy

Youcef Bekakra*, Djilani Ben Attous*

*Department of Electrical Engineering, University of El-Oued, P.O. Box 789, El-Oued 39000,

‡ Corresponding Author; Youcef Bekakra,University of El-Oued, Algeria, 213699098988,
youcef1984@gmail.com, dbenattous@yahoo.com

Received: 15.06.2012 Accepted:16.07.2012

Abstract- In this paper, we present a comparative study between space vector modulation (SVM) and pulse width modulation (PWM) inverter in sliding mode control (SMC) of active and reactive power control of a doubly fed induction generator (DFIG) for variable speed wind energy. The feasibility and effectiveness of the two methods are demonstrated by simulation results. The obtained results showed that, the proposed SMC with SVM inverter have stator and rotor current with low harmonic distortion and low active and reactive powers ripples than PWM inverter.

Keywords- Doubly Fed Induction Generator, Wind Energy, Sliding Mode Control, Space Vector Modulation, Pulse Width Modulation.

1. Introduction

The most important advantages of the variable speed wind turbines as compared with conventional constant speed system are the improved dynamic behavior, resulting in the reduction of the drive train mechanical stress and electrical power fluctuation, and also the increase of power capture [1]. One of the generation systems commercially available in the wind energy market currently is the doubly fed induction generator (DFIG) with its stator winding directly connected to the grid and with its rotor winding connected to the grid through a variable frequency converter. One of the most advantages of this system is that the rating of the power converter is one third of that of the generator [2]. With DFIG, generation can be accomplished in variable speed ranging from sub-synchronous speed to super-synchronous speed [3].

Through studying the characteristics of wind turbine, the paper proposed the maximum power point tracking (MPPT) control method. Firstly, according to the DFIG character, the paper adopts the vector transformation control method of stator oriented magnetic field to realize the decoupling control for the active power and reactive power using sliding mode control (SMC).

The sliding mode control theory was proposed by Utkin in 1977 [4]. Thereafter, the theoretical works and its applications of the sliding mode controller were developed. Since the robustness is the best advantage of a sliding mode control, it has been widely employed to control nonlinear systems that have model uncertainty and external disturbance [5].

Traditionally the sinusoidal pulse-width modulation (SPWM) technique is widely used in variable speed drive of induction machine, especially for scalar control where the stator voltage and frequency can be controlled with minimum online computational requirement. In addition, this technique is easy to implement. However, this algorithm has the following drawbacks. This technique is unable to fully utilize the available DC bus supply voltage to the VSI. This technique gives more total harmonic distortion (THD), this algorithm does not smooth the progress of future development of vector control implementation of ac drive.

These drawbacks lead to development of a sophisticated PWM algorithm which is Space Vector Modulation (SVM). This algorithm gives 15% more voltage output compare to the sinusoidal PWM algorithm, thereby increasing the DC bus utilization. Furthermore, it minimizes the THD as well as loss due to minimize number of commutations in the inverter [6].

In this paper, we apply the SMC method to the wind energy conversion systems of DFIG using the modulation strategy known as SVM technique and compared with the conventional PWM technique.

2. Space Vector Modulation

The underlying theory behind space vector modulation is to apply space vectors as illustrated in Fig. 1 for varying time periods in a pattern based on the SVM algorithm. Six space vectors can be obtained in a three phase system through six different combinations of open and closed switches in the inverter shown in Fig. 2. Only one switch may be closed per phase leg in order to prevent a short circuit. The space vectors represent the complex d-q voltage applied to the stator.

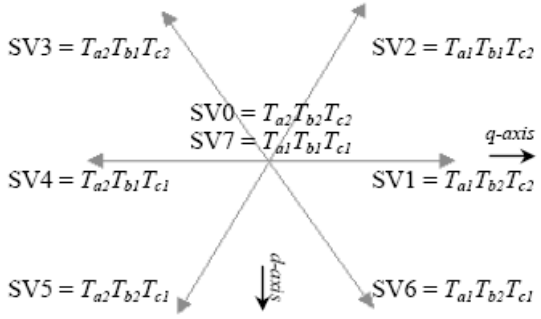

Fig. 1. Space vector d,q axis locations and their corresponding closed switches

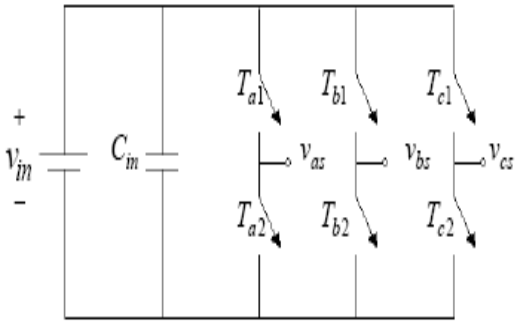

Fig. 2. Ideal three phase inverter

3. Model of Turbine

The wind turbine input power usually is [3]:

$$P_v = \frac{1}{2}\rho S_w v^3 \tag{1}$$

Where ρ is air density; S_w is wind turbine blades swept area in the wind; v is wind speed.

The output mechanical power of wind turbine is:

$$P_m = C_p P_v = \frac{1}{2} C_p \rho S_w v^3 \tag{2}$$

Where C_p represents the wind turbine power conversion efficiency. It is a function of the tip speed ratio λ and the blade pitch angle β in a pitch-controlled wind turbine. λ is defined as the ratio of the tip speed of the turbine blades to wind speed:

$$\lambda = \frac{R.\Omega_t}{v} \tag{3}$$

Where R is blade radius. Ω is angular speed of the turbine. C_p can be described as [7]:

$$C_p(\beta,\lambda) = (0.5\text{-}0.0167.(\beta\text{-}2)).sin(\frac{\pi.(\lambda+0.1)}{18.5\text{-}0.3.(\beta\text{-}2)}) \text{-}0.00184.(\lambda\text{-}3).(\beta\text{-}2) \tag{4}$$

4. Modelling of the DFIG

The general electrical state model of the induction machine obtained using Park transformation is given by the following equations [8]:

Stator and rotor voltages:

$$\begin{cases} V_{sd} = R_s.i_{sd} + \frac{d}{dt}\phi_{sd} - \omega_s.\phi_{sq} \\ V_{sq} = R_s.i_{sq} + \frac{d}{dt}\phi_{sq} + \omega_s.\phi_{sd} \\ V_{rd} = R_r.i_{rd} + \frac{d}{dt}\phi_{rd} - (\omega_s-\omega).\phi_{rq} \\ V_{rq} = R_r.i_{rq} + \frac{d}{dt}\phi_{rq} + (\omega_s-\omega).\phi_{rd} \end{cases} \tag{5}$$

Stator and rotor fluxes:

$$\begin{cases} \phi_{sd} = L_s.i_{sd} + M.i_{rd} \\ \phi_{sq} = L_s.i_{sq} + M.i_{rq} \\ \phi_{rd} = L_r.i_{rd} + M.i_{sd} \\ \phi_{rq} = L_r.i_{rq} + M.i_{sq} \end{cases} \tag{6}$$

The electromagnetic torque is done as:

$$C_e = pM(i_{rd}.i_{sq} - i_{rq}.i_{sd}) \tag{7}$$

and its associated motion equation is:

$$C_e - C_r = J\frac{d\Omega}{dt} \tag{8}$$

5. Field Oriented Control of DFIG

In this section, the DFIM model can be described by the following state equations in the synchronous reference frame whose axis d is aligned with the stator flux vector, ($\phi_{sd} = \phi_s$ and $\phi_{sq} = 0$) [9].

By neglecting resistances of the stator phases the stator voltage will be expressed by:

$$V_{sd} = 0 \text{ and } V_{sq} = V_s \approx \omega_s . \phi_s \quad (9)$$

We lead to an uncoupled power control; where, the transversal component i_{rq} of the rotor current controls the active power. The reactive power is imposed by the direct component i_{rd} .

$$P_s = -V_s \frac{M}{L_s} i_{rq} \quad (10)$$

$$Q_s = \frac{V_s^2}{\omega_s L_s} - V_s \frac{M}{L_s} i_{rd} \quad (11)$$

The arrangement of the equations gives the expressions of the voltages according to the rotor currents:

$$\dot{i}_{rd} = -\frac{1}{\sigma T_r} i_{rd} + g\omega_s i_{rq} + \frac{1}{\sigma L_r} V_{rd} \quad (12)$$

$$\dot{i}_{rq} = -\frac{1}{\sigma}\left(\frac{1}{T_r} + \frac{M^2}{L_s . T_s . L_r}\right) i_{rq} - g\omega_s i_{rd} + \frac{1}{\sigma L_r} V_{rq} \quad (13)$$

With:

$$T_r = \frac{L_r}{R_r} \; ; \; T_s = \frac{L_s}{R_s} \; ; \sigma = 1 - \frac{M^2}{L_s . L_r}$$

The system studied in the present paper is constituted of a DFIG directly connected through the stator windings to the network, and supplied through the rotor by a static frequency converter as presented in Fig. 3.

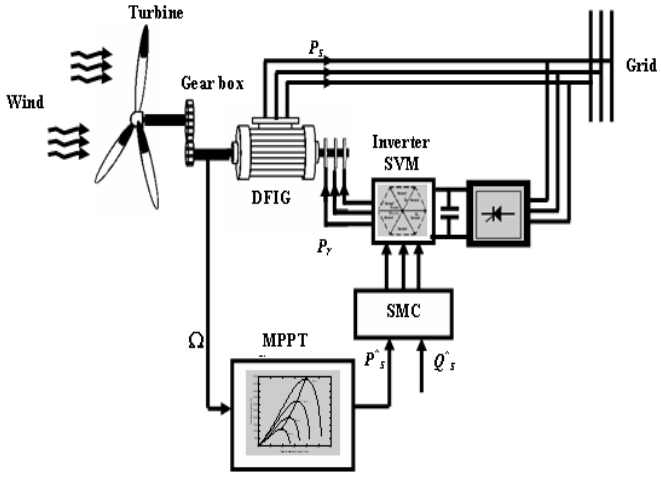

Fig. 3. DFIG variable speed wind energy conversion MPPT control

Where:

i_{rd} , i_{rq} are rotor current components, ϕ_{sd} , ϕ_{sq} are stator flux components, V_{sd} , V_{sq} are stator voltage components, V_{rd} , V_{rq} rotor voltage components. R_s and R_r are stator and rotor resistances, L_s and L_s are stator and rotor inductances, M is mutual inductance, σ is leakage factor and p is number of pole pairs. C_e is the electromagnetic torque, C_r is the load torque, J is the moment of inertia of the DFIM, Ω is mechanical speed, ω_s is the stator pulsation, ω is the rotor pulsation, f is the friction coefficient, T_s and T_r are statoric and rotoric time-constant.

6. Sliding Mode Control

The design of the control system will be demonstrated for a following nonlinear system [10]:

$$\dot{x} = f(x,t) + B(x,t).u(x,t) \quad (14)$$

Where $x \in \Re^n$ is the state vector, $U \in \Re^m$ is the control vector, $f(x,t) \in \Re^m$, $B(x,t) \in \Re^{n \times m}$.

From the system (14), it possible to define a set S of the state trajectories x such as:

$$S = \{x(t) \mid \sigma(x,t) = 0\} \quad (15)$$

Where:

$$\sigma(x,t) = \left[\sigma_1(x,t), \sigma_2(x,t), ..., \sigma_m(x,t)\right]^T \quad (16)$$

and $[.]^T$ denotes the transposed vector, S is called the sliding surface.

To bring the state variable to the sliding surfaces, the following two conditions have to be satisfied:

$$\sigma(x,t) = 0 \; , \quad \dot{\sigma}(x,t) = 0 \quad (17)$$

The control law satisfies the precedent conditions is presented in the following form:

$$\begin{aligned} u &= u^{eq} + u^n \\ u^n &= -k_f \, sgn(\sigma(x,t)) \end{aligned} \quad (18)$$

Where u is the control vector, u^{eq} is the equivalent control vector, u^n is the switching part of the control (the correction factor), k_f is the controller gain. u^{eq} can be obtained by considering the condition for the sliding regimen, $\sigma(x,t) = 0$. The equivalent control keeps the state variable on sliding surface, once they reach it.

For a defined function φ [11], [12]:

$$sgn(\varphi)=\begin{cases}1, & if\ \varphi>0\\ 0, & if\ \varphi=0\\ -1, & if\ \varphi<0\end{cases} \tag{19}$$

The controller described by the equation (18) presents high robustness, insensitive to parameter fluctuations and disturbances, but it will have high-frequency switching (chattering phenomena) near the sliding surface due to sgn function involved. These drastic changes of input can be avoided by introducing a boundary layer with width ε [10]. Thus replacing $sgn(\sigma(t))$ by $sat(\sigma(t)/\varepsilon)$ (saturation function), in (18), we have:

$$u = u^{eq} - k_f\, sat(\sigma(x,t)) \tag{20}$$

Where $\varepsilon > 0$:

$$sat(\varphi)=\begin{cases}sgn(\varphi), & if\ |\varphi|\geq 1\\ \varphi, & if\ |\varphi|<1\end{cases} \tag{21}$$

In this paper, we use the sliding surface proposed par J.J. Slotine,

$$\sigma(x,t)=\left(\frac{d}{dt}+\lambda\right)^{n-1} e \tag{22}$$

Where:

$x=\left[x,\dot{x},...,x^{n-1}\right]^T$ is the state vector,

$x^d=\left[x^d,\dot{x^d},...,x^d\right]^T$ is the desired state vector,

$e=x^d-x=\left[e,\dot{e},...,e^{n-1}\right]$ is the error vector, λ is a positive coefficient, and n is the system order.

7. Application of Sliding Mode Control to DFIG

The rotor currents (which are linked to active and reactive powers by equations (10) and (11), quadrature rotor current i_{rq} linked to active power P_s and direct rotor current i_{rd} linked to reactive power Q_s) have to track appropriate current references, so, a sliding mode control based on the above Park reference frame is used.

7.1. Quadrature Rotor Current Control with SMC

The sliding surface representing the error between the measured and reference quadrature rotor current is given by this relation:

$$e = i_{rq}^{\ *} - i_{rq} \tag{23}$$

For $n=1$, the speed control manifold equation can be obtained from equation (22) as follow:

$$\sigma(i_{rq}) = e = i_{rq}^{\ *} - i_{rq} \tag{24}$$

$$\dot{\sigma}(i_{rq}) = \dot{i_{rq}}^{*} - \dot{i_{rq}} \tag{25}$$

Substituting the expression of $\dot{i_{rq}}$ equation (13) in equation (25), we obtain:

$$\dot{\sigma}(i_{rq}) = \dot{i_{rq}}^{*} - \left(-\frac{1}{\sigma}\left(\frac{1}{T_r}+\frac{M^2}{L_S.T_s.L_r}\right)i_{rq} - g\omega_s i_{rd} + \frac{1}{\sigma L_r}V_{rq}\right) \tag{26}$$

We take:

$$V_{rq} = V_{rq}^{eq} + V_{rq}^{n} \tag{27}$$

During the sliding mode and in permanent regime, we have:

$$\sigma(i_{rq})=0,\ \dot{\sigma}(i_{rq})=0,\ \ V_{rq}^{n}=0$$

Where the equivalent control is:

$$V_{rq}^{eq} = \left(\dot{i_{rq}}^{*} + \frac{1}{\sigma}\left(\frac{1}{T_r}+\frac{M^2}{L_S.T_s.L_r}\right)i_{rq} + g\omega_s i_{rd}\right)\sigma L_r \tag{28}$$

Therefore, the correction factor is given by:

$$V_{rq}^{n} = k_{V_{rq}}\, sat(\sigma(i_{rq})) \tag{29}$$

$k_{V_{rq}}$: positive constant.

7.2. Direct rotor current control with SMC

The sliding surface representing the error between the measured and reference direct rotor current is given by this relation:

$$e = i_{rd}^{\ *} - i_{rd} \tag{30}$$

For $n=1$, the speed control manifold equation can be obtained from equation (22) as follow:

$$\sigma(i_{rd}) = e = i_{rd}^{\ *} - i_{rd} \tag{31}$$

$$\dot{\sigma}(i_{rd}) = \dot{i_{rd}}^{*} - \dot{i_{rd}} \tag{32}$$

Substituting the expression of $\dot{i_{rd}}$ equation (12) in equation (32), we obtain:

$$\dot{\sigma}(i_{rd}) = \dot{i}_{rd}^{*} - \left(-\frac{1}{\sigma T_r} i_{rd} + g\omega_s i_{rq} + \frac{1}{\sigma L_r} V_{rd} \right) \tag{33}$$

We take:

$$V_{rd} = V_{rd}^{eq} + V_{rd}^{n} \tag{34}$$

During the sliding mode and in permanent regime, we have:

$$\sigma(i_{rd}) = 0,\ \dot{\sigma}(i_{rd}) = 0,\ V_{rd}^{n} = 0$$

Where the equivalent control is:

$$V_{rd}^{eq} = \left(\dot{i}_{rd}^{*} + \frac{1}{\sigma T_r} i_{rd} - g\omega_s i_{rq} \right) \sigma L_r \tag{35}$$

Therefore, the correction factor is given by:

$$V_{rd}^{n} = k_{V_{rd}}\, sat(\sigma(i_{rd})) \tag{36}$$

$k_{V_{rd}}$: positive constant.

8. Simulation Results

The DFIG used in this work is a 4 kW, whose nominal parameters are indicated in the following:

Rated values: 4 kW, 220/380 V, 15/8.6 A.

Rated parameters: R_s = 1.2 Ω, R_r = 1.8 Ω, L_s = 0.1554 H, L_r = 0. 1568 H, M = 0.15 H, p = 2.

Wind turbine parameters are: R (Blade length) = 3 m, G (Gear) = 5.4.

Fig. 4.a and Fig. 5.a present the stator active power and its reference profiles injected into the grid using PWM and SVM respectively.

The stator reactive power and its reference profiles using PWM and SVM are presented in Fig. 4.b and 5.b respectively.

It is clear that the actual stator active power follows its desired using the two proposed controller incorporating PWM and SVM technique, and to guarantee a unity power factor at the stator side, the reactive power is maintained to zero.

Fig. 4.c and Fig. 5.c show the stator current and its zoom versus time respectively using PWM and SVM respectively.

Fig 4.d and Fig 5.d show the harmonic spectrum of output phase stator current obtained using Fast Fourier Transform (FFT) technique for PWM and SVM inverter respectively. It can be clear observed that all the lower order harmonics are reduced for SVM inverter (THD = 4.69%) when compared to PWM inverter (THD = 6.41%).

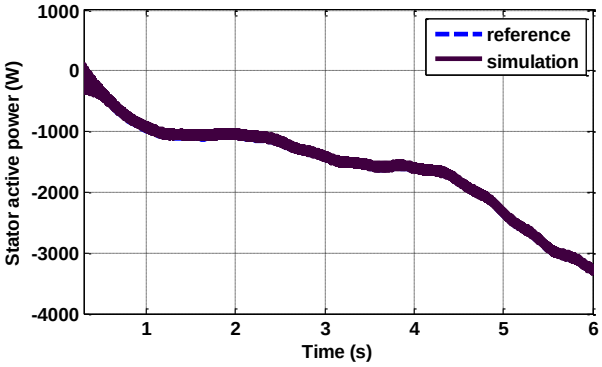

(a)

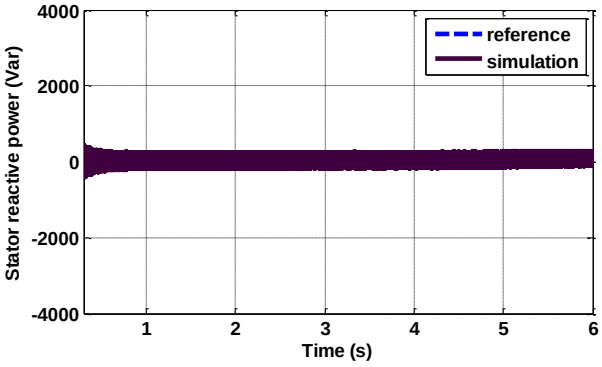

(b)

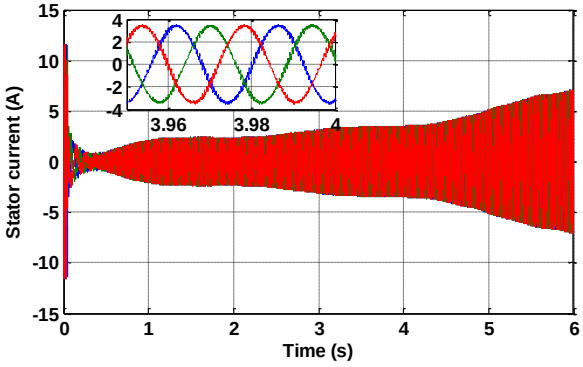

(c)

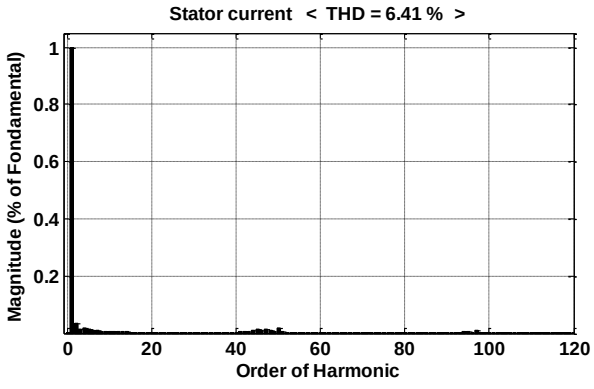

(d)

Fig. 4. (a) Stator active power, (b) reactive power, (c) stator current and (d) its spectrum harmonics using PWM

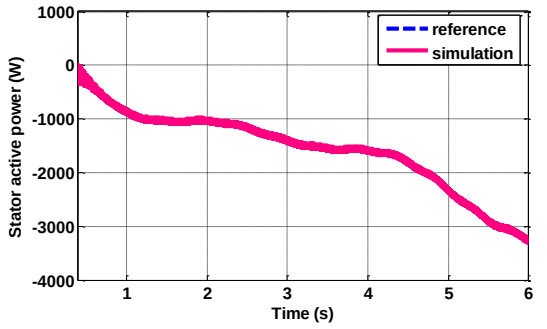

(a)

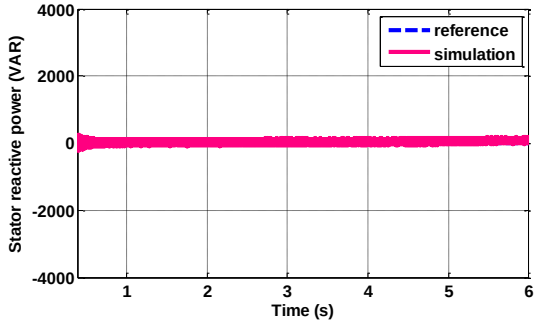

(b)

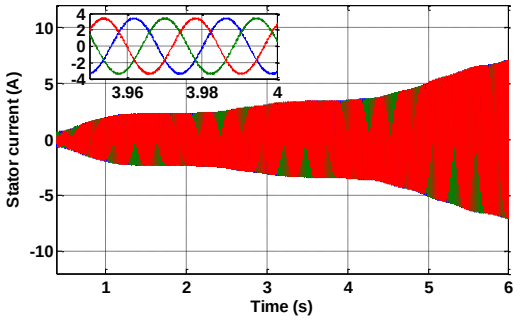

(c)

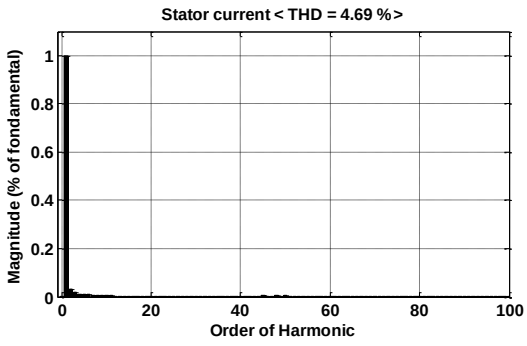

(d)

Fig. 5. (a) Stator active power, (b) reactive power, (c) stator current and (d) its spectrum harmonics using SVM

9. Conclusion

This paper presents simulation results of sliding mode control for active and reactive power control of a DFIG, using the modulation strategy of the SVM and PWM inverter. With results obtained from simulation, it is clear that for the same operation condition, the DFIG active and reactive power control with SMC using SVM technique had better performance than the PWM technique and that is clear in the spectrum of phase stator current harmonics which the use of the SVM technique, it is reduced of harmonics more than PWM technique.

References

[1] S. Heier, Grid integration of wind energy conversion systems, John Wiley and Sons; 1998.

[2] M. Verij Kazemi, A. Sadeghi Yazdankhah, H. Madadi Kojabadi, Direct power control of DFIG based on discrete space vector modulation, Renewable Energy, Vol. 35, pp. 1033-1042, 2010.

[3] J. Ik. Jang, Y. S. Kim, D. C. Lee, active and reactive power control of DFIG for wind energy conversion under unbalanced grid voltage, IPEMC, 2006.

[4] VI. Utkin, Variable structure systems with sliding modes-a survey. IEEE Trans. Automat Control,; Vol. 22, N°. 2, pp. 212-222, 1977.

[5] H. Amimeur, D. Aouzellag, R. Abdessemed, K. Ghedamsi, Sliding mode control of a dual-stator induction generator for wind energy conversion systems, Electrical Power and Energy Systems, Vol. 42, pp. 60-70, 2012.

[6] A. Jidin, T. Sutikno, MATLAB/SIMULINK based analysis of voltage source inverter with space vector modulation," TELKOMNIKA, Vol. 7, No. 1, pp. 23-30, April 2009.

[7] S. El Aimani, B. François, F. Minne, B. Robyns, Comparison analysis of control structures for variable speed wind turbine, In Proceedings of CESA, CD, Lille, France, July 2003.

[8] M. Machmoum, F. Poitiers, Sliding mode control of a variable speed wind energy conversion system with DFIG, International Conference and Exhibition on Ecologic Vehicles and Renewable Energies, MONACO, March 26-29 (2009).

[9] Y. Bekakra, D. Ben Attous, Sliding Mode Controls of Active and Reactive Power of a DFIG with MPPT for Variable Speed Wind Energy Conversion, Australian Journal of Basic and Applied Sciences, Vol. 5, N°. 12, pp. 2274-2286, 2011.

[10] Y. Bekakra, D. Ben attous, A sliding mode speed and flux control of a doubly fed induction machine, Electrical and Electronics Engineering, IEEE Conference, pp. I-174 - I-178, 2009.

[11] M. Abid, A. Mansouri, A. Aissaoui, B. Belabbes, Sliding mode application in position control of an induction machine, J. Electr. Engin., Vol. 59, N°. 6, pp. 322-327, 2008.

[12] J. Lo, Y. Kuo, Decoupled fuzzy sliding mode control, IEEE Trans. Fuzzy Syst., Vol. 6, N°. 3, pp. 426-435, 1998.